Paper presented at:
Ocean Optics Conference XXI, 8-12 Oct. 2012, Glasgow, Scotland

Utilizing Downwelling Irradiance for Phytoplankton Determination

Peter Gege

DLR, Earth Observation Center, Remote Sensing Technology Institute,
Oberpfaffenhofen, 82234 Wessling, Germany (peter.gege@dlr.de)

The downwelling irradiance is rarely utilized to determine optical parameters of a water body since the ever-changing water surface induces strong signal fluctuations in the upper meters of typically 20 to 40 %. An analytic model has been developed that calculates the spectra of the direct and diffuse component separately. It can cope with the fluctuations by treating, in addition to the unknown optical parameters of the water body, also the intensities of the two irradiance components as fit parameters during data analysis. The potential of this model for the determination of phytoplankton concentration was analyzed using data from two German lakes. Three phytoplankton classes could be identified above thresholds between 0.4 and 0.8 µg/l, and total pigment concentration (sum of chlorophyll-a and phaeophytin-a) could be determined with an uncertainty of 0.7 µg/l. This new approach may be of particular interest for shallow waters, where it is difficult to apply the usual reflectance-based algorithms due to bottom influences.

INTRODUCTION

Underwater measurements of downwelling irradiance (E_d) are rarely used directly for parameter retrieval since they depend much more on measurement and illumination conditions than reflectance which uses E_d for normalization of upwelling radiation. Figure 1 illustrates the strong dependency of E_d on depth (z), sun zenith angle (θ_{sun}) and on the relative intensities of the direct (f_{dd}) and diffuse (f_{ds}) irradiance components. The ever changing geometry of the water surface (waves, ripples, foam) leads to focusing and defocusing effects which change E_d intensity in the upper meters by typically 20 to 40 % (Dera and Stramski 1993, Hoffmann et al. 2008), but flashes can be an order of magnitude above average (Dera and Stramski 1986, Hieronymi and Macke 2012). The parameters f_{dd} and f_{ds} are used to model these wave focusing effects as described below.

In shallow waters, the upwelling radiation can be quite strongly influenced by the bottom. Reflection at the bottom adds wavelength and angle dependent contributions to the upwelling radiation which are usually not accurately known. Moreover, the intensity of this radiance contribution can be strongly variable since it captures the fluctuations of the downwelling radiation. The fluctuations do not cancel out for reflectance spectra since the upward and downward viewing instruments measure different light fields. Since E_d is much less affected by bottom effects than upwelling radiation, E_d based inversion algorithms could be an alternative to reflectance based methods to determine optical parameters of the water, at least in shallow areas. This expectation was the motivation of the current study.

To get an impression on the information content of E_d spectra concerning water constituents, figure 2 illustrates the changes of E_d caused by altered concentrations (C_4: dinoflagellates, X: suspended matter, Y: CDOM) and optical properties ($a^*(\lambda)$: specific absorption of phytoplankton, S: spectral slope of CDOM absorption). The paper investigates the capability of an E_d model for determining the concentrations of water constituents, with the focus on phytoplankton.

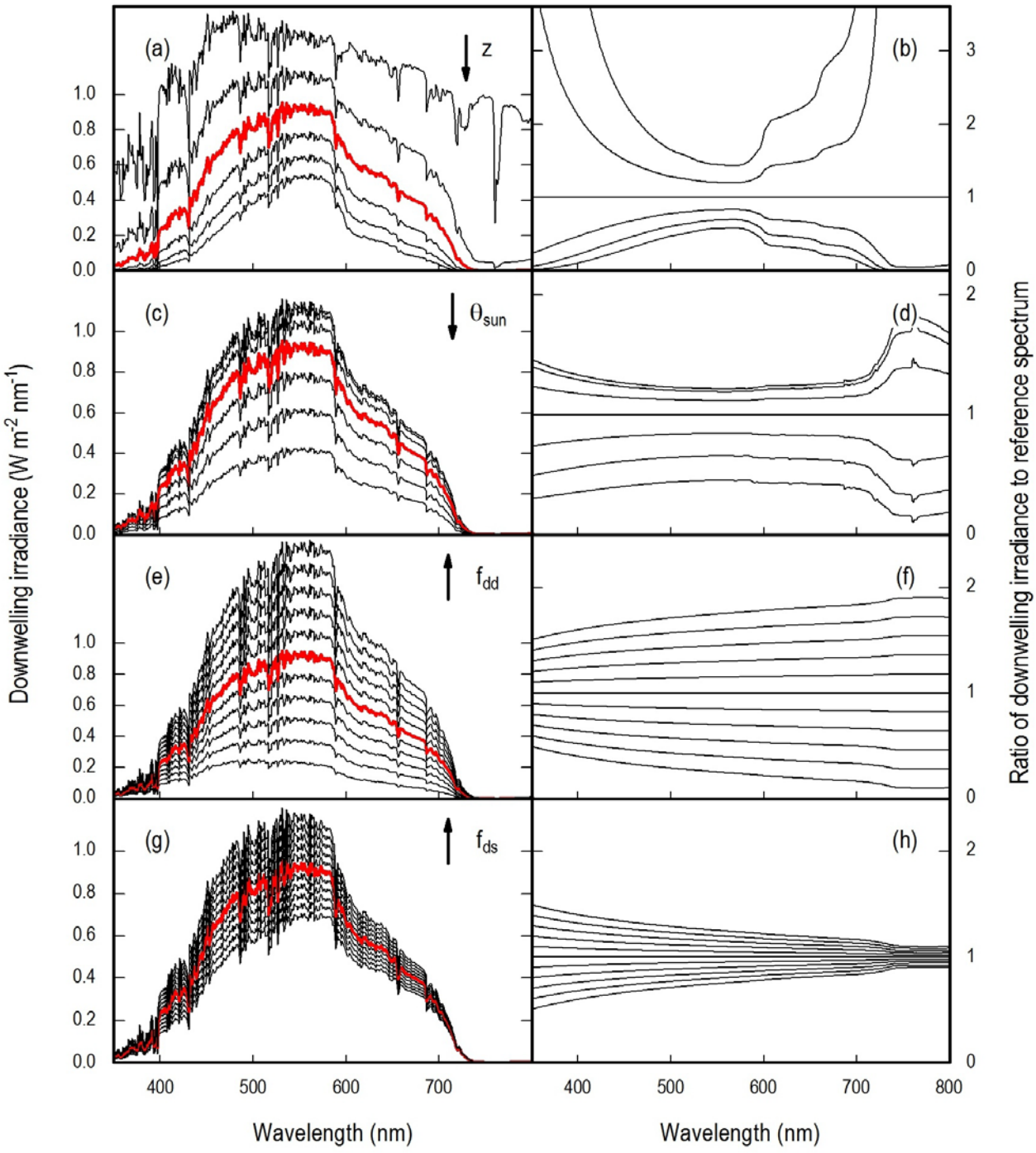

Figure 1: Dependency of E_d on measurement and environmental conditions. The red curves show the reference spectrum for z = 2 m, θ_{sun} = 30°, f_{dd} = 1, f_{ds} = 1. The left plots illustrate the absolute changes of E_d, the right plots the relative changes when a single parameter is altered: (a, b) z from 0 to 5 m, (c, d) θ_{sun} from 0 to 60°, (e, f) f_{dd} from 0 to 2, (g, h) f_{ds} from 0 to 2.

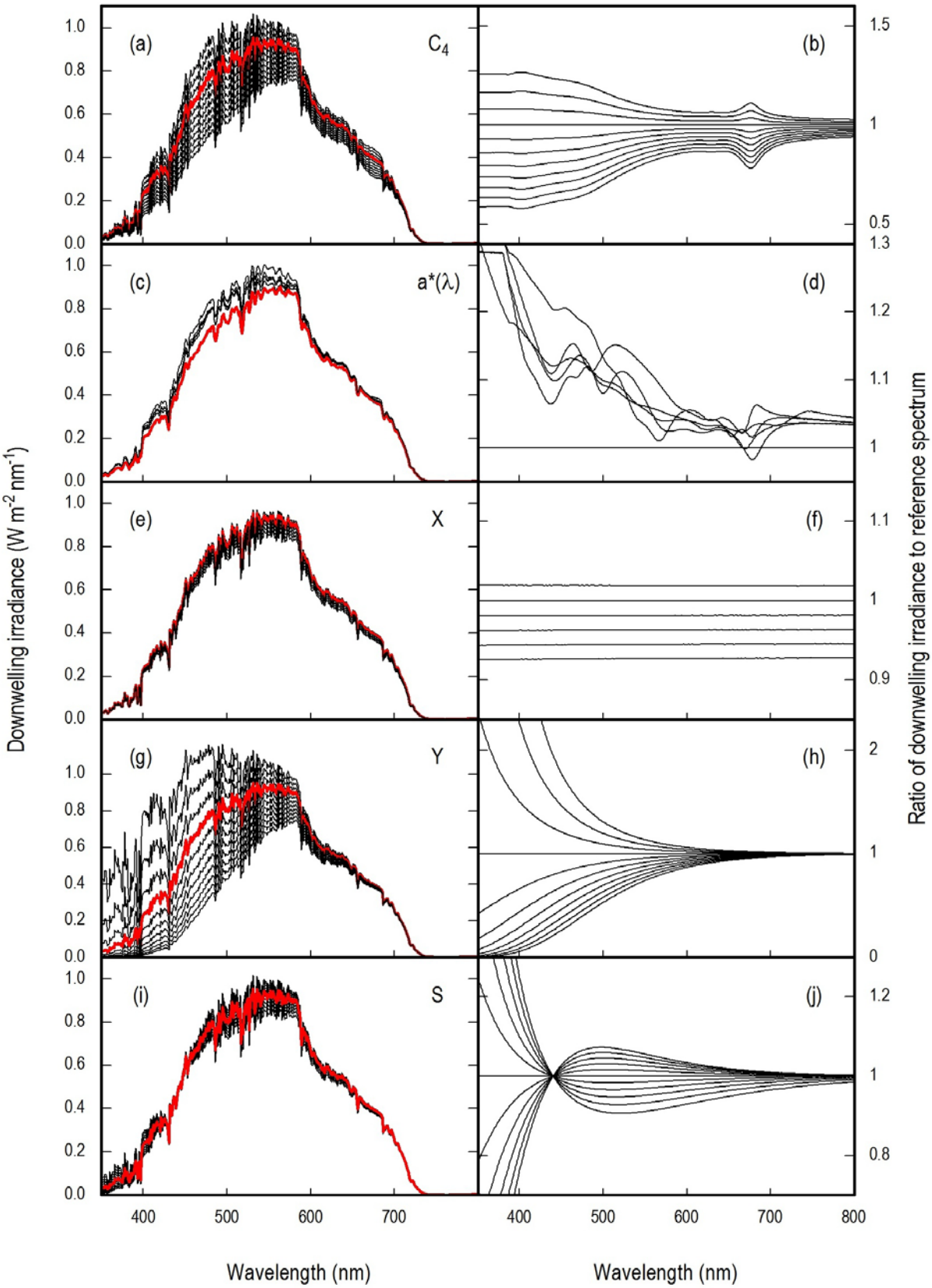

Figure 2: Dependency of E_d on water constituents. The red curves show the reference spectrum for z = 2 m, θ_{sun} = 30°, f_{dd} = 1, f_{ds} = 1, C_4 = 3 µg/l, X = 1 mg/l, Y = 0.3 m^{-1}, S = 0.015 nm^{-1}. The left plots illustrate the absolute changes of E_d, the right plots the relative changes when a single parameter is altered: (a, b) C_4 from 0 to 10 µg/l, (c, d) a*(λ) of 6 phytoplankton classes, (e, f) X from 0 to 5 mg/l, (g, h) Y from 0 to 1 m^{-1}, (i, j) S from 0.01 to 0.02 nm^{-1}.

IRRADIANCE MODEL

A depth-dependent analytic E_d model has been developed by Gege (2012) which can handle the described E_d variability by treating f_{dd} and f_{ds} as fit parameters during inverse modeling. It is summarized here briefly. The model distinguishes between the direct (E_{dd}) and the diffuse (E_{ds}) irradiance components and calculates total irradiance at depth z as follows:

$$E_d(\lambda, z) = f_{dd}E_{dd}(\lambda, z) + f_{ds}E_{ds}(\lambda, z). \quad (1)$$

λ denotes wavelength. The parameters f_{dd} and f_{ds} describe the intensities of E_{dd} and E_{ds} relative to conditions with a plane water surface. f factors < 1 correspond to intensity decrease, f factors > 1 to intensity increase.

The two components incident on the water surface, $E_{dd}(\lambda, 0+)$ and $E_{ds}(\lambda, 0+)$, are calculated using the analytic model of Gregg and Carder (1990). Their database was extended using Modtran calculations to cover the spectral range 300–1000 nm at a spectral resolution < 1 nm. The major parameters are sun zenith angle, ozone scale height, water vapor scale height, aerosol optical depth, and Angström exponent of aerosol scattering. The components at depth z are related to those above the water surface as follows:

$$E_{dd}(\lambda, z) = E_{dd}(\lambda, 0+)\exp\left\{-\frac{[a(\lambda)+b_b(\lambda)]z}{\cos\theta'_{sun}}\right\}(1-\rho_{dd}), \quad (2)$$

$$E_{ds}(\lambda,z) = E_{ds}(\lambda,0+)\exp\{-[a(\lambda) + b_b(\lambda)]zl_{ds}\}(1-\rho_{ds}). \quad (3)$$

ρ_{dd} and ρ_{ds} denote the reflectance factors of $E_{dd}(\lambda, 0+)$ and $E_{ds}(\lambda, 0+)$ at the water surface, respectively. They are calculated for a plane surface as a function of the sun zenith angle.

The path lengths of the two irradiance components are different. E_{dd} is a nearly parallel beam of light from the direction of the Sun, thus the path length is $z/\cos\theta'_{sun}$, where θ'_{sun} denotes the Sun zenith angle in water. In contrast, the rays forming E_{ds} originate from angles covering the entire upper hemisphere, hence their path lengths are very different. The resulting average path length is approximated as follows:

$$l_{ds} = 1.1156 + 0.5504(1-\cos\theta'_{sun}). \quad (4)$$

The optical properties of the water layer between surface and depth z are given by the absorption coefficient, a, and the backscattering coefficient, b_b. They are calculated as follows:

$$a(\lambda) = a_W(\lambda) + a_{ph}(\lambda) + a_Y(\lambda) + a_d(\lambda), \quad (5)$$

$$b_b(\lambda) = b_{b,W}(\lambda) + b_{b,X}(\lambda). \quad (6)$$

Pure water is characterized by its absorption coefficient, $a_W(\lambda)$, and its backscattering coefficient, $b_{b,W}(\lambda)$. The absorbing water constituents are characterized by their spectral absorption coefficients: phytoplankton by $a_{ph}(\lambda)$, coloured dissolved organic matter (CDOM) by $a_Y(\lambda)$, and non-algal particles (detritus) by $a_d(\lambda)$. Water constituents which scatter the light (suspended particles including phytoplankton cells) are represented by the spectral backscattering coefficient $b_{b,X}(\lambda)$.

IMPLEMENTATION

To apply the described irradiance model for data analysis, it has been implemented into version 4 of the software WASI (ftp://ftp.dfd.dlr.de/pub/WASI/). This tool has been developed for the simulation and inverse modeling of different types of spectral measurements in deep and shallow waters (Gege 2004, Gege and Albert 2006).

Since most measurements of this study are from lake Bodensee, and the other site, Starnberger See, is optically similar, the established bio-optical model of lake Bodensee (Heege 2000) was taken to represent the specific inherent optical properties (SIOPs). It neglects detritus absorption, $a_d(\lambda)$, and approximates backscattering of suspended particles by the wavelength-independent function $b_{b,X}(\lambda) = X b_{b,X}^*$ with X denoting concentration (mg/l) and $b_{b,X}^* = 0.0086$ m^2 g^{-1}. Phytoplankton is represented by the specific absorption spectra $a_i^*(\lambda)$ shown in Figure 3. If C_i denotes the concentration of class i (expressed as mass of chlorophyll-a plus phaeophytin-a, µg/l), the total absorption by phytoplankton is the following sum:

$$a_{ph}(\lambda) = \Sigma\, C_i\, a_i^*(\lambda). \qquad (7)$$

The normalized absorption spectrum of CDOM is usually approximated as $a_Y^*(\lambda) = \exp[-S(\lambda-\lambda_0)]$. This equation with different values of S is used below for sensitivity studies. For data analysis, the measured spectra shown in Figure 3 are used. The measurements from lake Bodensee have a spectral slope at 440 nm of 0.0100 ± 0.0025 nm^{-1} and those from Starnberger See of 0.0126 ± 0.0033 nm^{-1}; both have significantly higher absorption at λ > 500 nm than the exponential approximation would give. CDOM absorption is calculated as

$$a_Y(\lambda) = Y\, a_Y^*(\lambda), \qquad (8)$$

where Y is the absorption coefficient at $\lambda_0 = 440$ nm in units of m^{-1}.

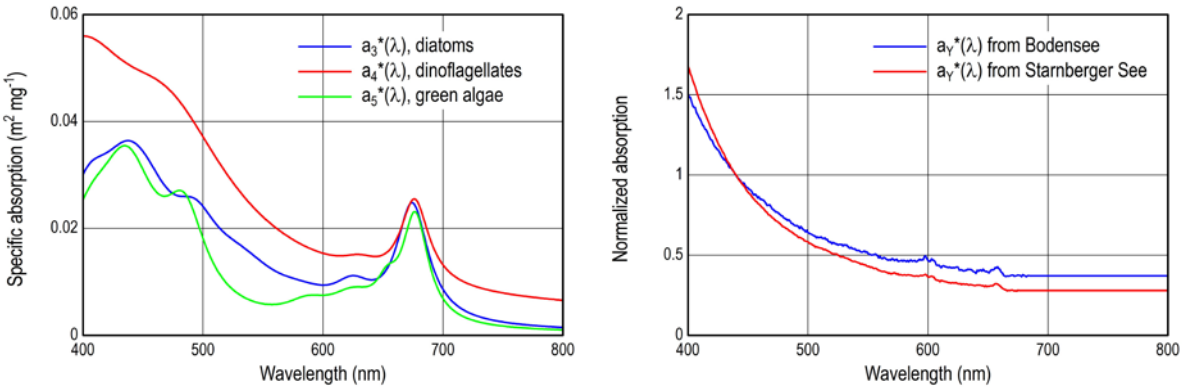

Figure 3: Specific absorption coefficients of phytoplankton (left) and CDOM (right).

INVERSE MODELING

Inverse modeling aims to determine the values of unknown parameters by fitting a model curve to the measured spectrum. This is done iteratively as follows. In the first iteration, a model spectrum $E_d(\lambda)$ is calculated using eq. (1) for user-defined initial values of the unknown model parameters (called fit parameters). This spectrum is compared with the measured one, $E_d^{meas}(\lambda)$, by calculating the residuum $\Sigma\, g_i\, |E_d^{meas}(\lambda_i) - E_d(\lambda_i)|^2$ as a measure of correspondence. Then, in the further iterations, the fit parameter values are altered, resulting in altered model curves and altered

residuals. The procedure is stopped when the calculated and the measured spectrum agree as good as possible, which corresponds to the minimum residuum. The values of the fit parameters of the final model curve are the fit results.

The parameters g_i of the residuum allow wavelength dependent weighting of the difference between measured and model curve, where $g_i = 1$ corresponds to the classical least squares fit. To amplify the spectral fingerprint of phytoplankton during inverse modeling, caused by chlorophyll-a absorption at 670 nm (Figure 2b), $g_i = 3$ is set in the range 610–750 nm and $g_i = 1$ otherwise.

An example of inverse modeling of a dataset is shown in Figure 4. 17 E_d measurements were made within 70 s at a constant sensor position in 1 m depth. Inverse modeling was carried out for each measurement. Two resulting model spectra are shown as red curves, the fit parameters and their standard deviations are given in the legend. In this example, inverse modeling determined the fit parameters *z*, *Y* and C_4 with low standard deviation, and C_3 and C_5 with large uncertainty, hence the concentrations C_3 and C_5 were too low for reliable detection. The observed high E_d variability was attributed mainly to intensity variations caused by wave focusing, expressed by high relative standard deviations of f_{dd} and f_{ds}.

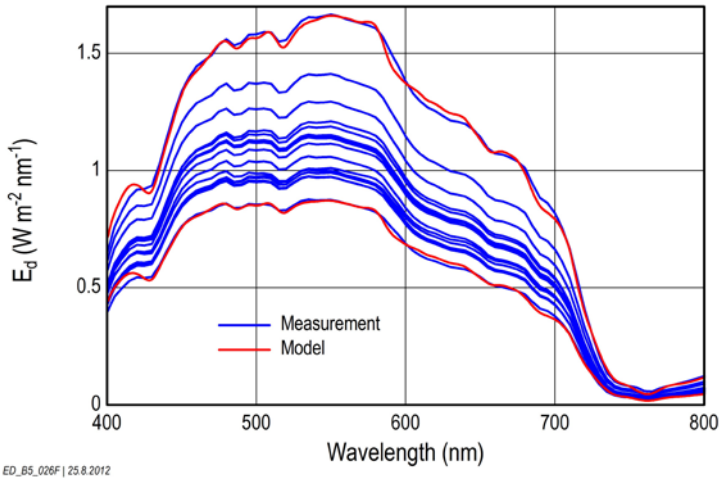

Figure 4: Illustration of inverse modeling. Average fit parameters of the 17 subsequent measurements: z = 1.01 ± 0.03 m, C_3 = 0.04 ± 0.12 µg/l, C_4 = 4.34 ± 0.42 µg/l, C_5 = 0.14 ± 0.11 µg/l, Y = 0.309 ± 0.009 m^{-1}, f_{dd} = 0.92 ± 0.24, f_{ds} = 1.56 ± 0.20.

RESULTS

A dataset of 407 measurements was collected in the German lakes Bodensee and Starnberger See at 74 stations mostly in shallow waters using a small boat (Pinnel 2007). Each measurement consisted of 4 to 50 individual E_d spectra from a RAMSES-ACC-VIS irradiance sensor (TriOS, Oldenburg, Germany) and accompanying water samples, which were analyzed for the concentrations of chlorophyll-a (*Chl-a*), phaeophytin-a (*Ph-a*) and total suspended matter (*X*), and for CDOM absorption ($a_Y(\lambda)$).

Inverse modeling requires initial values of the fit parameters. A reliable estimate can be made for *z* using the ratio E_d(800 nm) / E_d(680 nm) of the E_d measurement, see eq. (25) in Gege (2012), but the other parameters can have a large uncertainty. Thus, the sensitivity of the fit results on the initial values of the fit parameters was analyzed first. For that, inverse modeling was performed repeatedly for the complete dataset at altered initial values. The details are described in Gege (2013). The main results are:

- The initial value of X doesn't affect significantly the results of C_3, C_4, C_5, Y, S and z, but very much those of X, f_{dd} and f_{ds}. Consequently, the initial value choice of X is not critical for the fit results of phytoplankton, CDOM and sensor depth; however, X cannot be determined since f_{dd} and f_{ds} are not known. This is also obvious from Figure 2f: changes of X lead to wavelength-independent changes of E_d, like multiplying f_{dd} and f_{ds} with a common factor, see eq. (1).
- The initial values of C_3, C_4, C_5 affect slightly the fit results for C_3, C_4, C_5, but the fit results are consistent within a standard deviation.
- The initial value of Y affects both Y and S. That means, inverse modeling compensates Y errors by S errors and vice versa, i.e. concentration and spectral slope of CDOM cannot be reliably determined together; one of these parameters must be known.

In a second series of data analyses, the dependency of the fit results on S was investigated by repeating inverse modeling of all data with different fix S values. As a consequence of the previous results, in addition to S also X was kept constant. C_3, C_5 and z were not noticeably affected by the chosen S value, but very much C_4, Y, f_{dd} and f_{ds}. Consequently, the line shape of CDOM absorption needs to be known accurately to obtain reliable results for the concentrations of dinoflagellates and CDOM. The different behaviour of dinoflagellates to the other phytoplankton classes is caused by differences in their specific absorption spectra. As illustrated in Figure 3, diatoms and green algae have distinct spectral fine structures in the range from 400 to 500 nm, while the spectrum of dinoflagellates is smooth. Since it resembles CDOM absorption more than the other classes, it gets easier confused with CDOM during inverse modeling.

Taking those pitfalls into account, the dataset was analyzed concerning phytoplankton. Since X cannot be determined, X was set to the mean value of the in situ measurements, 1 mg/l, and kept constant during inverse modeling. Due to the importance of the spectral shape of CDOM absorption, the averaged laboratory spectra $a_Y^*(\lambda)$ of Bodensee and Starnberger See (Figure 3) were used instead of the S parameterization.

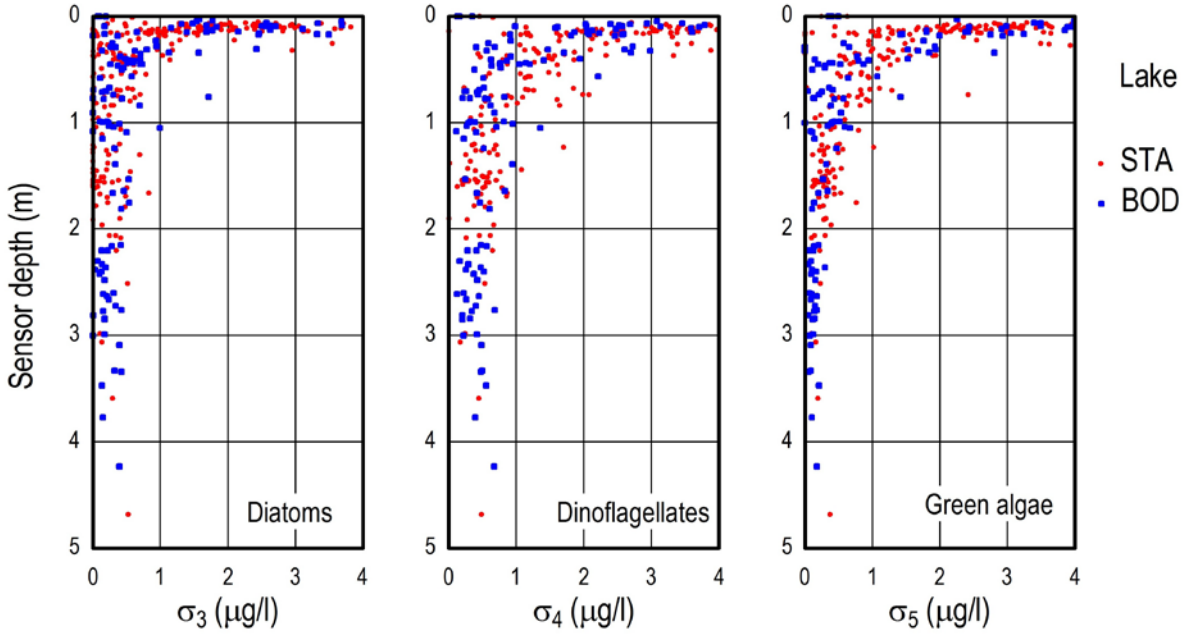

Figure 5: Standard deviation of phytoplankton concentration as a function of sensor depth.

Figure 5 shows the obtained standard deviations (σ) of C_3, C_4, C_5 as a function of sensor depth. σ can be very large close to the water surface and decreases approximately exponentially with z, reaching class-specific lower limits at depths between 1 and 1.5 m. Hence, the sensor must be at a depth of at least 1 to 1.5 m for accurate phytoplankton determination. For depths below 1.5 m, the standard deviations are on average σ_3 = 0.24 µg/l, σ_4 = 0.42 µg/l, σ_5 = 0.21 µg/l. For comparison, the concentration averages are C_3 = 0.29 µg/l, C_4 = 1.04 µg/l, C_5 = 0.75 µg/l. The increased standard deviations of dinoflagellates, σ_4, are caused by the variability of $a_Y^*(\lambda)$, which was not accounted for during data analysis since CDOM measurements were not available for each E_d measurement. By defining 2σ as threshold for detection and quantification, the threshold concentration is 0.5 µg/l for diatoms, 0.8 µg/l for dinoflagellates, and 0.4 µg/l for green algae.

Total pigment concentration is used to validate the derived concentrations since no class-specific *in situ* data are available. The comparison of the fit results, $C_3 + C_4 + C_5$, with the *in situ* values, *Chl-a + Ph-a*, is shown in Figure 6. All data from depths z > 1.5 m are used for the comparison (N = 68). Even though the concentration range of the dataset is small, the fit values are highly correlated to the *in situ* data. The correlation coefficient is r = 0.74, the standard deviation 0.66 µg/l.

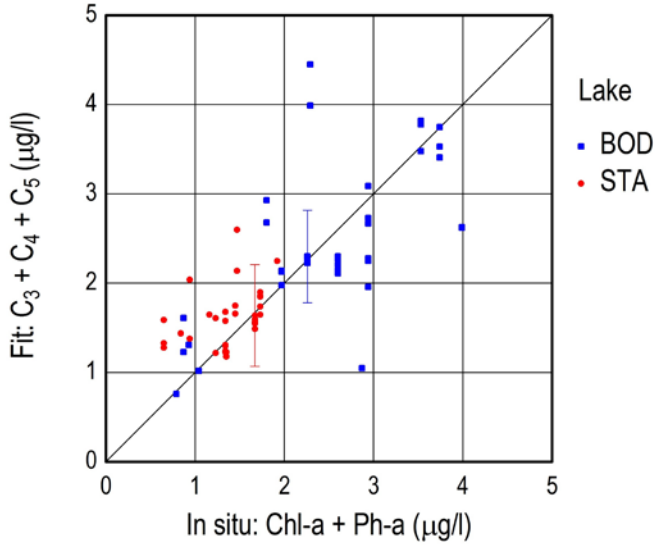

Figure 6: Pigment concentrations (chlorophyll-a + phaeophytin-a) of fit vs. in situ values. The error bars show the average standard deviation of the fit results for the two lakes.

SUMMARY AND CONCLUSIONS

The potential of a new analytic E_d model for estimating water constituent concentrations was analyzed in this study, with focus on phytoplankton concentration. The model can cope with the large and unpredictable fluctuations of the underwater light field, and it is insensitive to wavelength-independent errors of E_d, introduced for example by erroneous sensor calibration or changes of ρ_{dd} or ρ_{ds} caused by the geometry of the water surface, since the parameters f_{dd} and f_{ds} pick up such scaling effects during inverse modeling. For this study, no above-water measurements of E_d were available, but these would be helpful to improve E_d modeling under water.

It was found that the absorbing water constituents (CDOM, phytoplankton) can be determined from E_d measurements, but not the scattering components (suspended matter). The spectral shape of CDOM absorption plays a critical role. If it is not known accurately, it can lead to erroneous determination of CDOM and phytoplankton concentrations. Depending on the spectral shape of phytoplankton absorption, CDOM can be confused with phytoplankton. For the dataset analysed in

this study, CDOM strongly affected the retrieval accuracy of dinoflagellates, but only little that of diatoms and green algae.

At the test sites of this study, absorption at 440 nm was dominated by CDOM: *Y* ranged from 0.22 to 1.48 m^{-1}, and CDOM absorption exceeded that of phytoplankton on average by a factor of 6 at Bodensee and by a factor of 12 at Starnberger See. For these conditions, the water column above the sensor requires a thickness of at least 1 to 1.5 m for accurate phytoplankton determination. The threshold concentration to detect a phytoplankton class and to determine quantitatively its concentration was 0.4 µg/l for green algae, 0.5 µg/l for diatoms, and 0.8 µg/l for dinoflagellates. The uncertainty of total pigment concentration was 0.7 µg/l.

ACKNOWLEDGEMENT

All data used for this study were measured by Nicole Pinnel. She is acknowleged for providing the data and many stimulating discussions.

REFERENCES

J. Dera and D. Stramski (1986): Maximum effects of sunlight focusing under a wind-disturbed sea surface. *Oceanologia* **23**, 15–42.

J. Dera and D. Stramski (1993): Focusing of sunlight by sea surface waves: new results from the Black Sea. *Oceanologia* **34**, 13–25.

P. Gege (2004): The water colour simulator WASI: An integrating software tool for analysis and simulation of optical in-situ spectra. *Computers & Geosciences* **30**, 523–532.

P. Gege and A. Albert (2006): A tool for inverse modeling of spectral measurements in deep and shallow waters. *In: L. L. Richardson, E. F. LeDrew, eds. Remote Sensing of Aquatic Coastal Ecosystem Processes: Science and Management Applications.* Springer, pp. 81-109.

P. Gege (2012): Analytic model for the direct and diffuse components of downwelling spectral irradiance in water. *Applied Optics* **51**, 1407–1419.

P. Gege (2013): Estimation of phytoplankton concentration from downwelling irradiance measurements in water. *The Israel Journal of Plant Sciences*, accepted.

W. W. Gregg and K. L. Carder (1990): A simple spectral solar irradiance model for cloudless maritime atmospheres. *Limnol. Oceanogr.* **35**, 1657–1675.

T. Heege (2000): Flugzeuggestützte Fernerkundung von Wasserinhaltsstoffen am Bodensee. PhD thesis, FU Berlin. *DLR-Forschungsbericht* 2000-40, 134 pp.

M. Hieronymi and A. Macke (2012): On the influence of wind and waves on underwater irradiance fluctuations. *Ocean Science* **8**, 455–471.

H. Hofmann, A. Lorke, F. Peeters (2008): Wave-induced variability of the underwater light climate in the littoral zone. *Verh. Internat. Verein. Limnol.* **30**, 627–632.

N. Pinnel (2007): A method for mapping submerged macrophytes in lakes using hyperspectral remote sensing. PhD thesis. *Technical University Munich*, 165 pp.